Autoprecipitation Modelling in a Thickener

Daniel Rodrigues[1] and Robert LaMacchia[2]
1. Researcher
2. Research Consultant
Hydro, Belém, Brazil
Corresponding author: daniel.hco.rodrigues@hydro.com

Abstract

One of the principal alumina losses within the Bayer process is autoprecipitation or gibbsite reversion in the clarification circuit, yet rigorous modelling of this process remains poorly understood. This paper proposes a conceptual model for the autoprecipitation process within a clarification circuit decanter, considering the kinetics of the reaction within the complex solid-liquid separation environment. The model discretizes a Bayer process decanter into N stages with each stage comprising mixing, reaction, and splitting, while adhering to, a typical depth versus solids concentration profile. A degrees of freedom analysis to ensure that the models results are possible is presented. A batch of simulations are shown to demonstrate the impact of process variables such as feed volumetric flow, underflow solids concentration, and feed A/C ratio on the ratio drop of both underflow and overflow of the thickener.

Keywords: Gibbsite reversion, autoprecipitation, mud thickener, modelling.

1. Introduction

Typically, the objective of a refinery's red side is to deliver filtered green liquor with as high alumina concentration as acceptable to the white side, considering product quality, operability, type of equipment, etc. The higher the alumina concentration attained, the greater the propensity to lose it during the thickening of the blow-off slurry. While the optimal A/C ratio can be discovered through operation experience, a more structured way to do this would be using a model that accurately represents the complex behavior of the thickeners, including solids profile, liquor composition, temperature, and residence time.

The gibbsite reversion (or autoprecipitation) phenomenon has been studied by multiple authors in the past [1] [2] [3] [4] [5]**,** arriving at a good level of agreement concerning the contributing factors.. The solids concentration affects the process but so too does the mineral composition of the solids. In that regard, the literature agrees that goethite is the second most influential mineral on the enhancement of the autoprecipitation rate, after gibbsite. These results regarding the mineral impact are consistent with results reported by researchers from the Kirkvine refinery [3], in which aluminous goethite was found to play an important role in gibbsite reversion. A correlation between the specific alumina loss through autoprecipitation has been estimated based on the goethite to alumina ratio [2] has also been encountered and used for estimate of the bauxite composition impact on the losses. Additionally, insights regarding mechanisms of gibbsite precipitation on foreign surfaces have been studied through in-situ X-ray diffraction shown by Webster et Al. [4] [5] demonstrating both diffusion controlled bidimensional crystal growth and unidimensional diffusion in different conditions, more representative of a scale growth condition.

Quantitative modelling of this process has been less explored. In [6] the kinetics of this reaction was estimated experimentally in the laboratory in conditions similar to batch reactors. Their kinetic data was applied to a model that simulated the reaction in a Plug-Flow Reactor inside the thickener geometry. The base kinetic equation used is Equation 1.

$$\frac{dA}{dt} = k \cdot (A - A^*)^{2.28} \cdot FC^{-4.21} \cdot (0.195 + I)^5 \cdot e^{-0.957 \cdot I} \quad (1)$$

$$k = k_0 \cdot e^{\left(-5470\left(\frac{1}{T} - \frac{1}{T_0}\right)\right)} \quad (2)$$

Where:

A is the concentration of alumina in g Al_2O_3/L;
A^* is the Alumina solubility in g Al_2O_3/L;
FC is the free caustic concentration in g Na_2CO_3/L;
I is the Ionic strength in mol/L;
k is the rate constant ($g^{2.93} \cdot L^{2.07} \cdot mol^{-5} \cdot h^{-1}$);
k_0 is the rate constant at the reference temperature;
T_0 is the reference temperature in K;
T is the temperature in K;

Poor agreement of the experimental data with the plant was encountered, but even so, the model was capable of guiding a reported reduction on alumina loss of 80 % in lead washers. The model did not take the solids concentration and composition into account, and the experimental procedure included sieving and ring milling of dried mud collected from settle underflow which can affect the surface area available for autoprecipitation. In an earlier approach from 1986, J.G. Lepetit [2] suggested that the kinetics have two different terms based on the autoprecipitation of both gibbsite and boehmite. The kinetic equation utilized was:

$$\frac{dRP}{dt} = -k_3 \cdot (RP - RPe_3)^2 - k_1 \cdot (RP - RPe_1)^2 \quad (3)$$

$$k_1 = a_1 \cdot m \cdot e^{(-\alpha \cdot I - \frac{E_1}{R \cdot T} + \beta_1)} \quad (4)$$

$$k_3 = a_3 \cdot m \cdot e^{(-\alpha \cdot I - \frac{E_3}{R \cdot T} + \beta_3)} \quad (5)$$

Where:

RP is the ponderal ratio expressed by g Al_2O_3/g Na_2O;
RPe_3 and RPe_1 are ponderal ratios at solubility for gibbsite and boehmite respectively;
k_3 and k_1 are the kinetic constants;
β_3, β_1, and α are terms independent of the processed red muds;
a_3 and a_1 are terms that represent the processed red mud;
m is the solids concentration in g/L;
E_3 and E_1 are the activation energies;
I is the Ionic strength;
R is the ideal gas constant;

The results from this study were in better agreement with plant data, but with less capacity as we move down the washer train, as it is observable in **Table *1***.

Table 1. Comparison between model and plant data, as studied by J.G. Lepetit [2].

Unit	Plant RP	Calculated Rp
Thickener	1.100	1.100
Washer 1	1.043	1.035
Washer 2	0.907	0.921
Washer 3	0.814	0.835
Washer 4	0.724	0.718

Washer 5	0.591	0.619
Washer 6	Not determined	0.553

Based on the reported reductions of alumina loss, modelling of this phenomena is the target of this work for future optimization of Alunorte's clarification circuit. The effect of different solids concentration throughout the vessel has not been explored in prior work, nor have the kinetic approaches reported considered the solids composition impact. The model proposed needs to be able to take both the behavior of the thickener and the kinetics of the process into account such as to inherently be affected by the solids profile and result into two different liquor streams on the overflow and underflow of the thickener.

2. Methodology

2.1. Model Concept

Regarding a thickener model, multiple assumptions need to be made. Solids move continuously toward the bottom of the tank and the slurry density (Figure 1) increases following the same direction. Similarly, the liquid generally flows in the direction of the overflow with smaller streams generated from the lower part of the tank caused by the densification of solids, which "purge" the liquor that is in between the particles. Accordingly, mixing is happening all throughout the height of the vessel.

To represent all of the effects occurring throughout the vessel, this work proposes a compartmentalization of the thickener sections such that stages under and over the feed height exist. Excluding the top and bottom compartments of the model, all others are fed with a stream coming from the stages above, and below, and if necessary a feed stream. Concurrent with this approach, every compartment produces two streams that feed the stages above and below. . In this work, the first section is counted as the one that is at the top, with the incremented moving toward the underflow (see **Figure 1**). Both the first stages and last stages only have one feeding stream, as they do not have the adjacent stages and they are the source of the overflow and underflow of the thickener streams. The index used to identify the streams refer to the stage from which they are leaving.

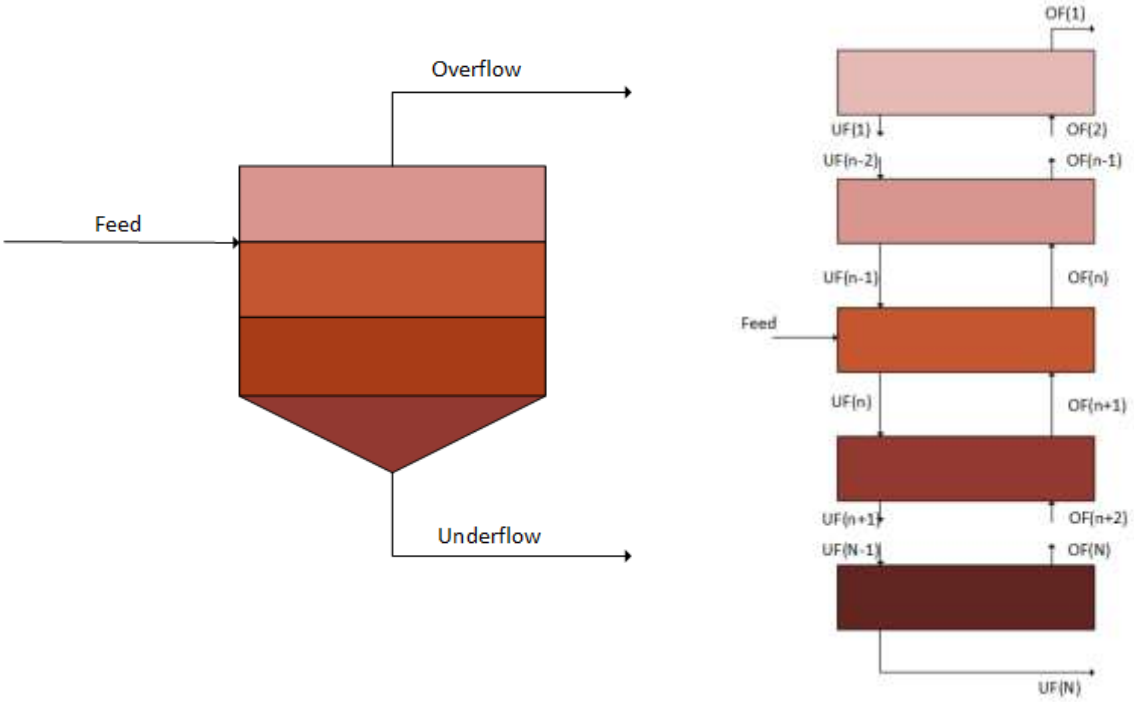

Figure 1. Model schematic for a thickener unit.

Every compartment is then represented by three operations, a Mixer, a Reactor and a Splitter, as represented in Figure 2 where the reactor is based on the CSTR model.

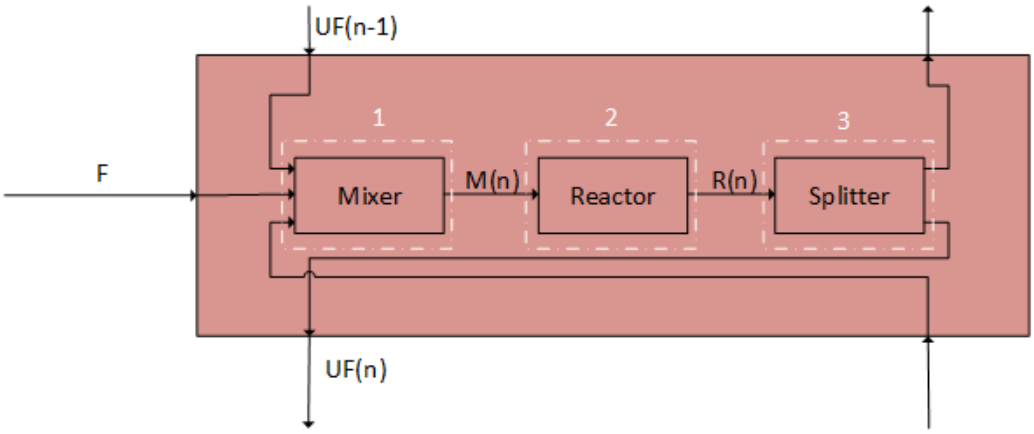

Figure 2.Representation of the internal operations of each compartment.

2.2. Degrees of Freedom Analysis

For a set of N stages with feed on stage "f", "l" components in the liquor phase and "s" components in the solid phase, the mass balances on the interface between operations is done by the following set of equations. For the mixer:

$$F + UF_{n-1} + OF_{n+1} = M_n \tag{6}$$

$$F \cdot \alpha(F) + UF_{n-1} \cdot \alpha(UF_{n-1}) + OF_{n+1} \cdot \alpha(OF_{n+1}) = M_n \cdot \alpha(M_n) \tag{7}$$

$$F \cdot \alpha(F) \cdot x_i(F) + UF_{n-1} \cdot \alpha(UF_{n-1}) \cdot x_i(F) + OF_{n+1} \cdot \alpha(OF_{n+1}) \cdot x_i(F) = M_n \cdot \alpha(M_n) \cdot x_i(F) \tag{8}$$

$$F \cdot \big(1-\alpha(F)\big)\cdot y_j(F) + UF_{n-1}\cdot\big(1-\alpha(UF_{n-1})\big)\cdot y_j(F) + OF_{n+1}\cdot\big(1-\alpha(OF_{n+1})\big)\cdot y_j(F) = M_n\cdot(1-\alpha(M_n))\cdot y_j(F) \quad (9)$$

Where the "F" refers to total mass flow of the feed stream, "α(S)" is the liquor mass fraction of the "S" stream, "UF_n" is the total mass flow of the underflow coming from the nth stage, "OF_n" is the total mass flow of the overflow leaving the nth stage, "$x_i(S)$" is the mass fraction of the i^{th} component of the liquor phase in the "S" stream, "$y_j(S)$" is the mass fraction of the j^{th} component of the solid phase in the "S" stream, and "M_n" is the total mass flow of the stream leaving the Mixer. For the reactor:

$$M_n = R_n \quad (10)$$
$$M_n\cdot\alpha(M_n) = R_n\alpha(R_n) + \Delta R(n) \quad (11)$$
$$M_n\cdot\alpha(M_n)\cdot x_i(M_n) = R_n\cdot\alpha(R_n)\cdot x_i(R_n) + \Delta R_i(n) \quad (12)$$
$$M_n\cdot(1-\alpha(M_n))\cdot y_j(M_n) = R_n(1-\alpha(R_n))\cdot y_j(R_n) + \Delta R_j(n) \quad (13)$$

Where the new terms are the total mass flow leaving the reactor on the n^{th} stage "R_n", the impact of the reaction on the liquor mass flow of stage n "ΔR(n)", the impact of reactions on the i^{th} component of the liquor phase on the n^{th} stage "$\Delta R_i(n)$", and the impact on the j^{th} component of the solids phase on the n^{th} stage "$\Delta R_j(n)$". For the Splitting stage:

$$R_n = UF_n + OF_n \quad (14)$$
$$R_n\cdot\alpha(R_n) = UF_n\cdot\alpha(UF_n)\cdot + OF_n\cdot\alpha(OF_n) \quad (15)$$
$$R_n\cdot\alpha(R_n)\cdot x_i(R_n) = UF_n\cdot\alpha(UF_n)\cdot x_i(UF_n) + OF_n\cdot\alpha(OF_n)\cdot x_i(OF_n) \quad (16)$$
$$R_n\cdot\big(1-\alpha(R_n)\big)\cdot y_j(R_n) = UF_n\cdot(1-\alpha(UF_n))\cdot y_j(UF_n) + OF_n\cdot(1-\alpha(OF_n))\cdot y_j(OF_n) \quad (17)$$

Where no new term is presented. All of the variables as described here as are summarized in **Table *2***. Calculation of the reaction terms are essential, but not to the summary in the table.

Table 2. Summary of all possible variables in a thickener model stage with s solid components and l liquid components.

Variables						
F	UF_{n-1}	OF_{n+1}	M_n	R_n	UF_n	OF_n
α(F)	$\alpha(UF_{n-1})$	$\alpha(OF_{n+1})$	$\alpha(M_n)$	$\alpha(R_n)$	$\alpha(UF_n)$	$\alpha(OF_n)$
$x_1(F)$	$x_1(UF_{n-1})$	$x_1(OF_{n+1})$	$x_1(M_n)$	$x_1(R_n)$	$x_1(UF_n)$	$x_1(OF_n)$
$x_2(F)$	$x_2(UF_{n-1})$	$x_2(OF_{n+1})$	$x_2(M_n)$	$x_2(R_n)$	$x_2(UF_n)$	$x_2(OF_n)$
...	...	...	...	...	...	...
$x_l(F)$	$x_l(UF_{n-1})$	$x_l(OF_{n+1})$	$x_l(M_n)$	$x_l(R_n)$	$x_l(UF_n)$	$x_l(OF_n)$
$y_1(F)$	$y_1(UF_{n-1})$	$y_1(OF_{n+1})$	$y_1(M_n)$	$y_1(R_n)$	$y_1(UF_n)$	$y_1(OF_n)$
$y_2(F)$	$y_2(UF_{n-1})$	$y_2(OF_{n+1})$	$y_2(M_n)$	$y_2(R_n)$	$y_2(UF_n)$	$y_2(OF_n)$
...	...	...	...	...	...	...
$Y_s(F)$	$Y_s(UF_{n-1})$	$Y_s(OF_{n+1})$	$Y_s(M_n)$	$Y_s(R_n)$	$Y_s(UF_n)$	$Y_s(OF_n)$

Giving us a total of 7×(2+s+l) variables on each stage where the "2" refer to the total mass flow and liquor mass fraction mass balances and the "7" is the number of possible streams on each stage. That expression is representative of one stage, but when the whole system is analyzed, if we simply multiply the expression by the amount of stages a number of variables would be double counted. For that reason, the correct expression for the number of variables is:

$$\#Var = (2 + l + s) \cdot (5N + 2) \quad (18)$$

On the equations side, for each stage we have 3 unit operations with total mass balances, liquor mass balances, l-1 component mass balances on the liquor phase and s-1 component mass balances on the solid phase, yielding:

$$\#Eqs = 3 \cdot (s + l) \cdot N \quad (19)$$

The specification of the feed stage conditions will specify all of the correct stage feed variables and determine all of the other stages' Feed streams as zero. With the addition of the UF(0) and OF(N+1) as non-existent, and the determination of the liquor fraction of each OF and UF stream based on a user-given solids profile, the number of specifications are.

$$\#ProcessSpecs = (3 + l + s) \cdot (2 \cdot N) \quad (20)$$

As for restrictions, in each splitting step there is no change in composition of each phase, only a difference between the liquor fraction of each, giving N×(s+l) restrictions. For all of the streams other than feed streams we have by definition $\sum x_i = 1$ and $\sum y_i = 1$, but special care must be taken because two of the OF and UFs , for each stage, are already accounted for in the other stages and the leaving OF and UF have the same composition, making this pair linearly dependent. Accordingly:

$$\#Restrictions = 8N + N \cdot (s + l) \quad (21)$$

The total degrees of freedom is calculated through:

$$DegreesOfFreedom = \#Var - (\#Eqs + \#ProcessSpecs + \#Restrictions) = 0 \quad (22)$$

This analysis therefore establishes that the system can in fact be solved for any numbers of liquor and solids components, as long as the reaction kinetics are known.

2.3. Model Simulated Conditions

For this model proof of concept, the assumptions were as follows:

- Steady State Mass Balance;
- All of the precipitation occurs through growth and follows King's SPR [7] with a k0 of 1000. The final expression takes into account the size change of particles using the equation:

$$\frac{dGibb}{dt} = k_0 \cdot e^{-\frac{E}{R \cdot T}} \cdot C_S^{\frac{2}{3}} \cdot \left(\frac{(A - A^*)^2}{FC}\right) \quad (23)$$

- There is no solids differentiation in the residue and precipitation occurs in the same rate for both gibbsite and residue solids fractions;
- Liquor density is calculated through the Mulloy-Donaldson correlation [8];
- Nortier's gibbsite solubility correlation is used [9] [10];
- Mixing and Separation have ideal behavior;
- CSTR reactor;
- Two linear solids profiles, one ranging from feed density to overflow density and another ranging from feed density to underflow density based on height of the stage starting from feed stage to overflow or underflow (Figure 3);

- Feed Volumetric Flow ranging from 850 – 1350, Feed A/TC Ratio ranging from 0.700 – 0.800, Thickener UF Solids ranging from 15 % – 25 %, and number of stages ranging from 3 – 20;
- Temperature at 95 °C, OF solids fraction is 0.01 %, feed solids mass fraction is 5 %, and TC at the feed is 293 g Na_2CO_3/L;
- Thickener Volume is 1200 m³ and it is cylindrical with every stage having equal volume;
- The model is solved using SysCAD 9.3 and associated customized PGM files to reflect the above.

A total of 749 simulations were run to evaluate the model performance and stability with repetitions starting from different initializations as a form of gauging the capacity of the model to give a unique solution for a unique condition.

3. Results

The simulation results for A/C 0.800, Volumetric feed flow of 1100 m³/h, and UF solids of 20 % and changing only the number of stages used to represent the total volume showed that the number of stages does influence the resulting streams, specially regarding UF properties. This is clearly seen in Figure 4**,** which shows the ratio drop from the feed to the OF and UF. The slope of these changes reduces with the number of stages, which suggests that there is a number of stages that can be considered essentially stable. Obviously, this will depend on both the feed conditions and the relevant kinetic equations used. Note that the kinetic equation shown here is purely for demonstrative concepts and has not been rigorously verified. For the impact of process variables on the results, the simulations shown have 20 stages which is the maximum number of stages simulated here and only one variable will be changed keeping all others constant, using as a base Feed A/C Ratio of 0.800, Feed Volumetric flow of 1100 m³/h and a solids UF mass fraction of 20 %. Feed solids concentration should affect the process as different seeds change the precipitation rate, but the simplification on kinetics expressions will not evaluate that effect as the expression is only taking total solids concentration as argument. In reality, alumina concentration on the solids is of high importance.

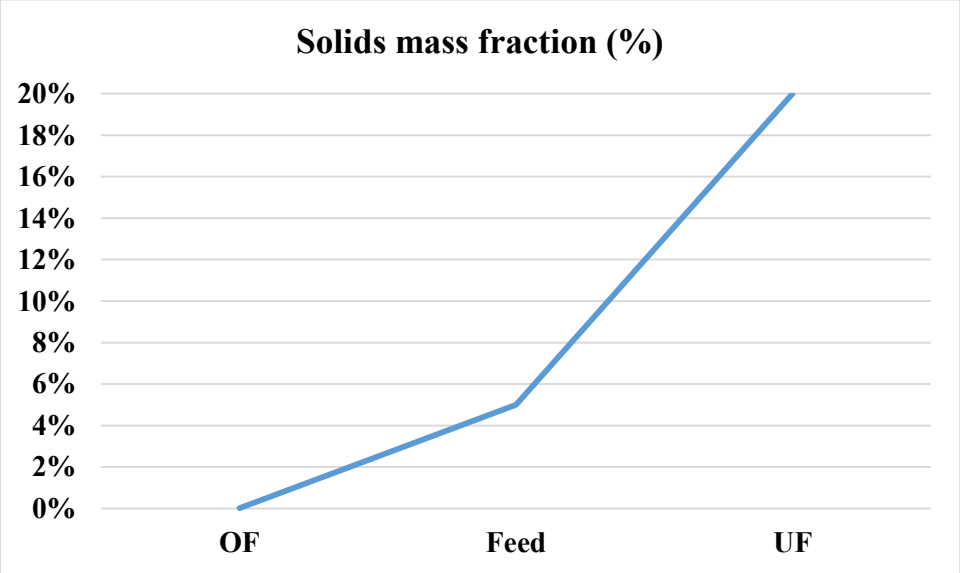

Figure 3. Example solids (%) profile inside the thickener based on OF, Feed and UF parameters.

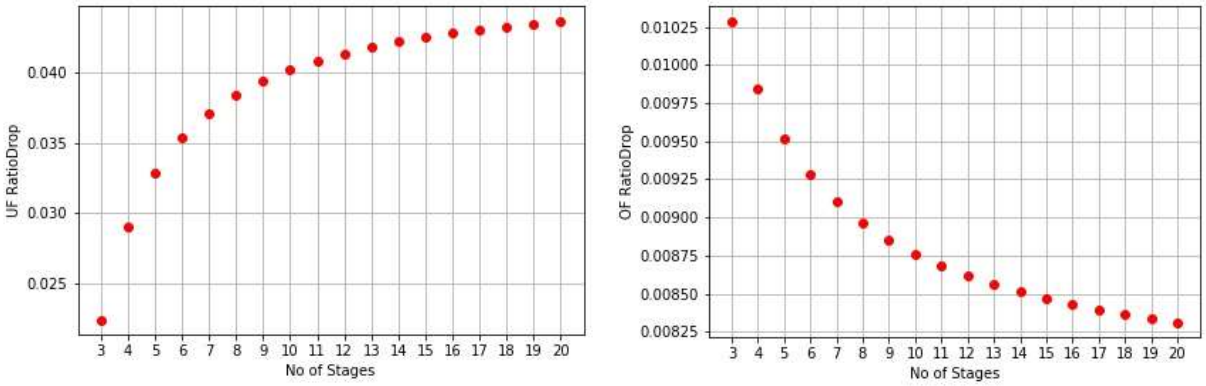

Figure 4. OF and UF ratio drop from the feed A/C ratio when the number of stages used in the model changes.

The same ratio drop is strongly influenced by the feed A/C ratio. Both OF and UF are almost linearly affected by that change, but the slope of that effect is different, being the one on UF much more evident.

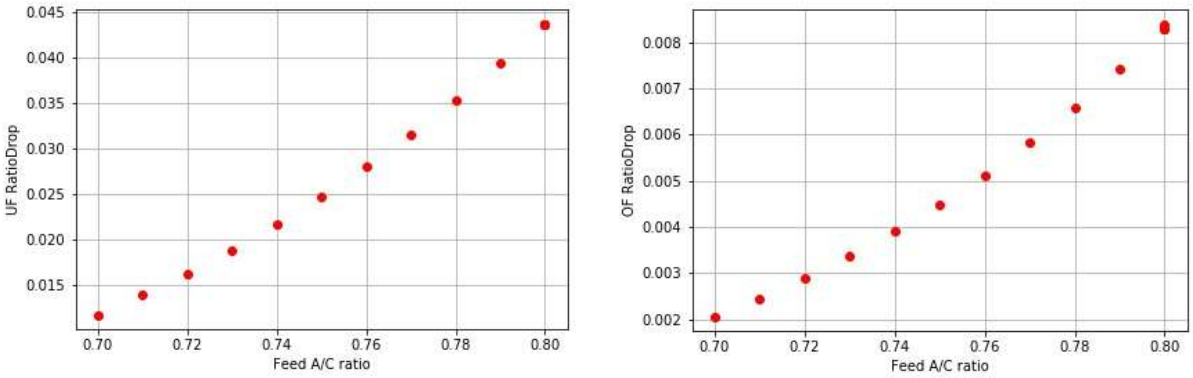

Figure 5. OF and UF ratio drop from the feed A/C ratio when changing the feed A/C ratio.

The opposite trend occurs when the volumetric flow is the one variable changed, but the effect of the UF ratio drop is still much stronger (Figure 6). Finally, the effects of increasing the UF solids concentration is observed in Figure 7, showing that the higher the UF solids concentration, the higher the ratio drop is, with a difference on the impact if observing different streams. Note that in the simulations where conditions were feed A/C = 0.800, Feed Volumetric flow is 1100 m³/h and UF Solids Conc. is 20 %, there is more than one point in Figure 5, **Error! Reference source not found.**, and **Error! Reference source not found.**. For stability reasons these simulations were run multiple times from different starting points to ensure that the final results were approximately the same, which they are.

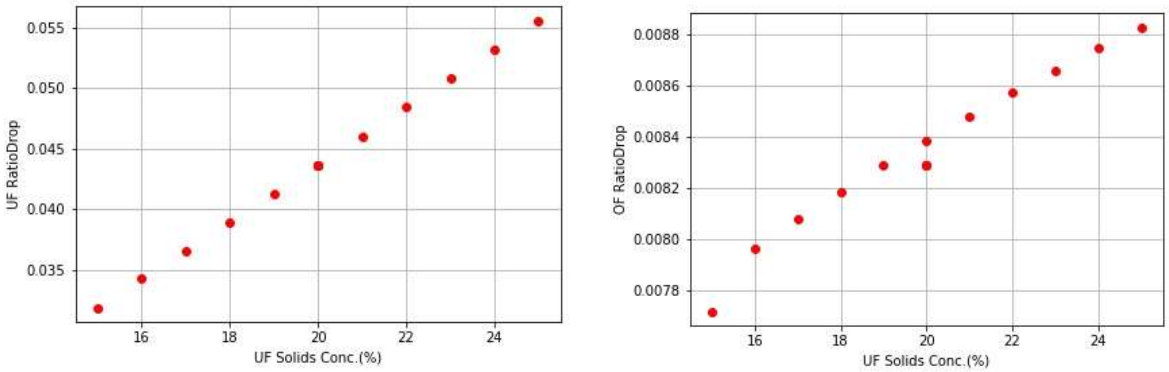

Figure 6. OF and UF ratio drop from the feed A/C ratio when changing the feed volumetric flow.

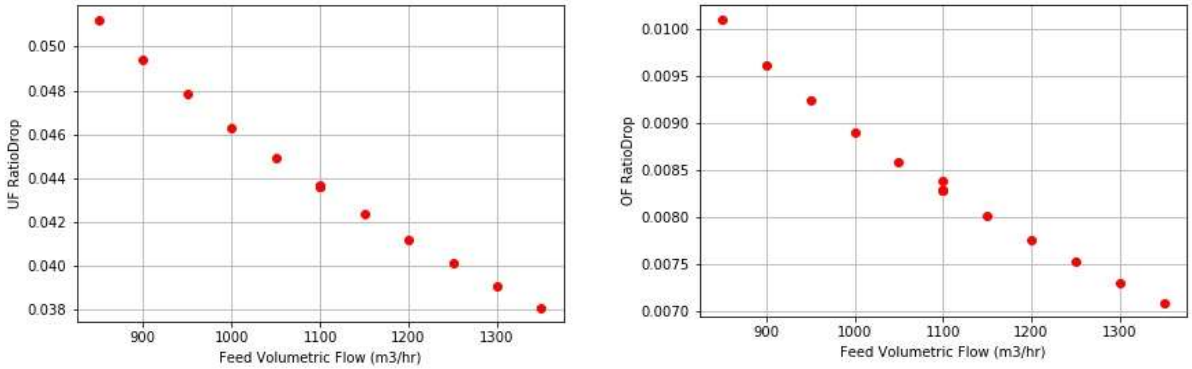

Figure 7. OF and UF ratio drop from the feed A/C ratio when changing the UF solids

4. Discussion

Regarding number of stages, there is a decrease in difference between results at every stage added (**Error! Reference source not found.**). The variation in the impact for every increment of stages is not the same in the OF and UF streams. As the UF stream shows a higher slope of change, it was used as a reference for the analysis of this impact. At 17 stages, the difference between every increment starts being negligible for the cases simulated here on the basis that it is less than 0.001 ratio point, typically used as the smallest measurable increment. It is also noticeable that when a low number of stages is used, the ratio drop estimated is higher than with more stages in the OF but lower than estimated in the UF. When rebuilding the mass balances of the solids phase leaving the underflow, that might cause a bias on the gibbsite content and create the perception that the model might not represent the phenomenon correctly when plant data is used for evaluation. It can also cause wrong estimates of optimal process variables if the model is used for modelling of the whole clarification circuit. A straight consequence of this analysis is that before the utilization of this model for actual modelling exercises on the refinery, the number of stages used must be analyzed for each tank before the total modelling.

The effect of process variables can be observed clearly, even if we use a nonsensical kinetic expression. The results follow an intuitive trend for the feed A/C ratio, causing a high impact on

how much autoprecipitation affects the leaving streams. The underflow is much more impacted and that agrees with the fact that most of the solids are in fact in the bottom part of the tank and the amount of liquor present on that region is smaller, which attest to the fact that the impact should be higher. These results are a consequence of the larger supersaturation degree. The impact of increasing volumetric feed flow is also intuitive as a straight consequence is the reduction of residence time, giving the material less time to auto precipitate. Again, the effect of the variable is more relevant on the underflow and the cause is the larger solids concentration in the bottom of the tank, similar to the effect of the feed A/C ratio. The UF solids concentration change affects the slope of the region under the feed stage, which means that the total solids content of the tank is changed. If the UF solids increase, then the total amount of solids inside the tank should increase. Note here that the mud and interface level are not considered as these definitions are simply a reference of a specific point of the solids profile. Being so the model takes into account the mud and interface levels just by receiving the input of the solids profile and the increase of the UF solids concentration as done in this work has the consequence of raising both the interface and mud levels. The oversimplified solids profile is again part of the effort of proving concept with the simplest conditions. There are numerous studies which define the typical solids profiles (see for example [11] [12] [13] [14] [15] [16] [17]) and these represent the next logical improvement for the model. Further, with better evaluated kinetics considering different precipitation mechanisms and solids composition, the effects of the solids profile and residue composition can be estimated prior to operation if needed.

5. Conclusions

The proposed model adequately represents with stable results the expected tendencies of the process when certain parameters are manipulated. This refers to the fact that the ratio drop on both OF and UF increases when feed A/C ratio increases and decreases when feed volumetric flow increase. It naturally differentiates the liquor compositions of the overflow and underflow leaving the thickener. The number of stages influences the result and for this proof of concept 20 stages was enough, but depending on the process conditions (and kinetic equations utilized) the number of stages may not be the same. The model here developed is not only useful for autoprecipitation modelling but for any reaction that happens inside a thickener and for any number of components as the degrees of freedom analysis is 0 independently of number of components so long as the kinetics of each modelled reaction are known. The impact of different solid compositions can be considered in the model by using different kinetic expressions implemented on the reactor step for each solid component interference, if the information is available. The suggested following work is to validate kinetic expressions extracted through bench experiments and confirmation of applicability using plant data, observing the impact of different solid compositions and solid mass fraction profiles. After careful modelling of plant data, the obvious next step will be process optimization and control using these methods.

6. Acknowledgements

DR thanks Dr. Domingos Fabiano Santana Souza from the Federal University of Rio Grande do Norte., for the fruitful discussions, guidance and support throughout the development of this model. Both authors extend thanks to Hydro for the permission to execute and publish this work.

7. References

1. T. Harato, T. Ishida, and K. Yamada, Autoprecipitation of gibbsite and boehmite. In *Proceedings of the Light Metals* (Dallas 1982), 141-147.

2. J. G. Lepetit,. Autoprecipitation of alumina in the Bayer process. In *Proceedings of the Light Metals* 1986 (New Orleans 1986), 225-230.
3. Keddon Andre Powell, Luke J. Kirwan, Kieran Hodnett, Desmond Lawson, Ab Rijkeboer, Characterisation of alumina and soda losses associated with the processing of goethitic rich Jamaican bauxite. In *The Proceedings of the Light Metals* (San Fancisco 2009), 151-156.
4. Nathan A. S. Webster, Ian C. Madsen, Melissa J. Loan, Robert B. Knott, Fatima S. Naim, Kia S. Wallwork and Justin A. Kimpton, An investigaion of goethite-seeded Al(OH)3 precipitation using in situ X-ray diffraction and Rietveld-based quantitative phase analysis. *Journal of Applied Crystallography* (2010), 466-472.
5. Nathan A. S. Webster, Melissa J. Loan, Ian C. Madsen, Robert B. Knott, and Justin A. Kimpton. An investigation of the mechanisms of goethite, hematite and magnetite-seeded Al(OH)3 precipitation from synthetic Bayer liquor. *Hydrometallurgy* (2011), 72-79.
6. M. Kiriazis, Settler and Washer Alumina Reversion. *In Proceedings of the 7th International Alumina Quality Workshop* (Perth 2005), 123-126.
7. W. R. King, Some studies in alumina trihydrate precipitation kinetics. In *Proceedings of the Light Metals* (1973), 551-563.
8. SysCAD, “Alumina 3 Bayer Species Model,” SysCAD, 18 May 2017. [Online]. Available: https://help.syscad.net/index.php?title=Alumina_3_Bayer_Species_Model. [Accessed 24 May 2018].
9. P. Nortier, P. Chagnon, and A. E. Lewis, Corrigendum to "Modelling the solubility in Bayer liquors: A critical review and new models” *Chem. Eng. Sci.* 66 (2011) 2596-2605. *Chem. Eng. Sci.* (2013), 3519.
10. P. Nortier, P. Chagnon, and A. E. Lewis, Modelling the solubility in Bayer liquors: A critical review and new models. *Chemical Engineering Science* (2011), 2596-2605.
11. P. Bürger, M. C. Bustos, and F. Concha, Settling velocities of particulate systems: 9. Phenomenological theory of sedimentation processes: numerical simulation of the transient behavior of flocculated suspensions in an ideal batch or continuous thickener. *International Journal of Mineral Processing*, 55 (November 1999), 267-282.
12. R. Bürger and F. Concha, Mathematical model and numerical simulation of the settling of flocculated suspensions. *International Journal of Multiphase Flow*, 24 (May 1998), 1005-1023.
13. R. Bürger, A. García, K. H. Karlsen, and J. D. Towers, A kinematic model of continuous separation and classification of polydisperse suspensions. *Computers and Chemical Engineering*, 32 (May 2008), 1173-1194.
14. P. Garrido, R. Burgos, F. Concha, and R. Bürger, Settling velocities of particulate systems: 13. A simulator for batch and continuous sedimentation of flocculated suspensions. *International Journal of Mineral Processing*, 73 (April 2004), 131-144.
15. Mehdi Rahimi, Ali A. Abdollahzadeh, and Bahram Rezai, Dynamic Simulation of Tailing thickener at the Tabas coal washing plant using the phenomenological model. *International Journal of Mineral Processing*, 154 (July 2016), 35-40.
16. Shane P. Usher, Rudolph Spehar, and Peter J. Scales, Theoretical analysis of aggregate densification: Impact on thickener performance. *Chemical Engineering Journal*, 151 (February 2009), 202-208.
17. Ben B. G. van Deventer, Shane P. Usher, Ashish Kumar, Murray Rudman, and Peter J. Scales, Aggregate densification and batch settling. *Chemical Engineering Journal*, 171 (March 2011), 141-151.